

# Three-Point Bending Test and Finite Element Simulation Study of 304 Stainless Steel Based on Elastoplastic Constitutive Model

Di Yan, Nan Yang, Chong Fu\*, Haiying Feng

*Henan Institute of Metrology, Zhengzhou, Henan, China*

*\*Corresponding Author*

**Abstract:** Rebar bending is commonly found in engineering and has received widespread attention. In this paper, a combination of experimental and finite element methods was used to conduct a study on three-point bending of 304 stainless steel. The real-time bending angle of the round bar during bending was recorded using a digital inclinometer. The force-displacement curves of specimens with different diameters were obtained and compared with the results of finite element simulations. Furthermore, the results from the digital inclinometer were compared with theoretical angle values. The findings suggest that the larger the diameter of the 304 stainless steel round bar, the greater the normal force it experiences. The finite element results are relatively consistent with the experimental results. The angle displayed by the digital inclinometer is consistent with the theoretical angle value of the round bar before unloading. The rebound angle of the reinforcing bar is greatly influenced by its diameter. When the diameter of the round bar exceeds a certain value, the rebound angle can be neglected.

**Keywords:** Three-point Bending; Bending Angle; Finite Element Simulation; 304 Stainless Steel

## 1. Introduction

Rebar bending is one of the main processes in rebar processing, usually using bending and pulling methods to bend rebars into different shapes and size specifications<sup>[1]</sup>. Rebar bending and shaping are mainly accomplished by horizontal rebar bending machines and vertical rebar bending machines<sup>[2]</sup>. The precision of rebar bending has a significant impact on its engineering application, and researchers have conducted extensive studies in this area. Yan found through experiments

that when the bending angle is  $<180^\circ$ , bending controlled by displacement is feasible<sup>[3]</sup>; Chen et al. developed an application program relating the experimental press head travel to the angle so as to avoid errors in angle measurement during bending tests, thus improving the accuracy of the test detection<sup>[4]</sup>; Zheng et al., based on the finite element model of vertical rebar bending, used the orthogonal test method to analyze the factors affecting the rebound angle and further modified the formula for the rebound angle<sup>[5]</sup>.

The three-point bending test is commonly used to detect the bending mechanical properties of materials. Hu et al., based on the virtual crack model, proposed an analytical method for calculating the instability fracture toughness of rebar concrete three-point bending beams<sup>[6]</sup>; Wang et al., through static three-point bending loading tests, explored the influence of the PVA fiber content on the bending performance of PVA fiber-reinforced composite beams<sup>[7]</sup>. In addition, the three-point bending test, combined with a digital angle ruler, can achieve real-time bending angle measurement of the component<sup>[8]</sup>.

In this paper, three-point bending tests were conducted on 304 stainless steel round bars of different diameters. The bending angles of the round bars were recorded using a digital inclinometer and compared with the theoretical angle values calculated based on the press head displacement and the round bar size. A three-point bending model of the 304 stainless steel round bar was established using finite element software and compared with the experimental force-displacement curve.

## 2. Methods and Theory

### 2.1 Experimental Materials and Methods

A dynamic and static material property analysis test system (WPS-25H) was used to conduct three-point bending tests on 304

stainless steel round bars with lengths of 200mm and diameters of 4, 6, 8, and 10mm, as shown in Figure 1. The distance  $d$  between the two supports was 120mm. Each diameter of the round bar was tested three times. The press head used a displacement loading method, with a pressing speed  $v$  of 5mm/min and a depth  $h$  of 30mm. The force-displacement curve was obtained during this process, and the bending angle of the round bar was recorded in real-time using a digital inclinometer.

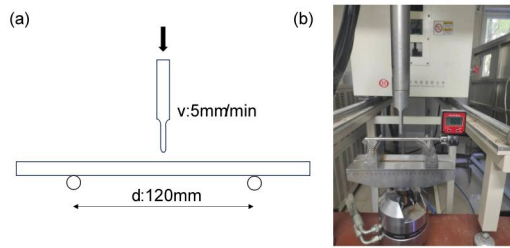


**Figure 1. Three-Point Bending Test. (A) Schematic Diagram of Three-Point Bending, (B) Three-Point Bending Test Diagram.**

A uniaxial tensile test was performed on 304 stainless steel with a specimen size of a straight round bar with a gauge length of 25 mm and a diameter of 6 mm. The uniaxial tensile test used MTS Landmark 370.25, with a displacement loading rate of 1mm/min. The obtained stress-strain curve was fitted to determine the elastic modulus  $E$ , yield strength  $\sigma_y$ , and strain hardening index  $n$  of the 304 stainless steel material, which were then input into the finite element model.

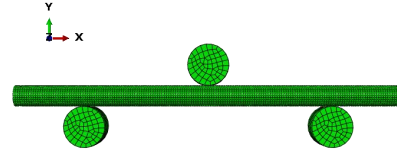
### 2.2 Finite Element Simulation

Figure 2 shows the three-point bending model established in the ABAQUS finite element software. The indenter and the three-point bending support columns are both cylindrical bodies with a radius of 10mm and a height of 15mm, both set as rigid bodies. The process of rebar bending is a complex elastoplastic deformation problem. Taking into account the nonlinear characteristics of the material [9], the power law hardening constitutive model is used to assign the material properties of the round bar, as shown in equation (1) [10].

$$\begin{cases} \sigma = E \varepsilon, & \varepsilon \leq \varepsilon_y, \\ \sigma = E \varepsilon_y^{1-n} \varepsilon^n & \varepsilon > \varepsilon_y, \end{cases} \quad (1)$$

The diameters of the round bars are 4mm, 6mm, 8mm, and 10mm, with a length of 200mm each. The three-point bending support columns of the model are fully constrained,

fixing the degrees of freedom in the z-direction of the round bar and the rotation around the x and y directions. The mesh type of the entire model is C3D8R. The loading conditions are consistent with the experiment.

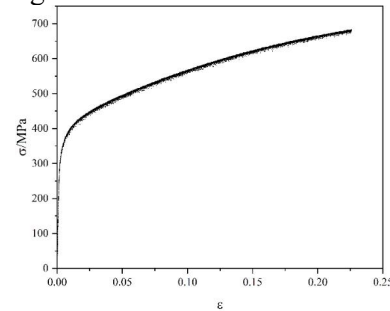


**Figure 2. Finite Element Model of Three-point Bending.**

## 3. Results and Discussion

### 3.1 Experimental Results

Figure 3 shows the true stress-strain curve of the 304 stainless steel material. The elastic modulus of the material is found to be 195GPa, with a yield strength of 343.2MPa and a hardening index of 0.24.



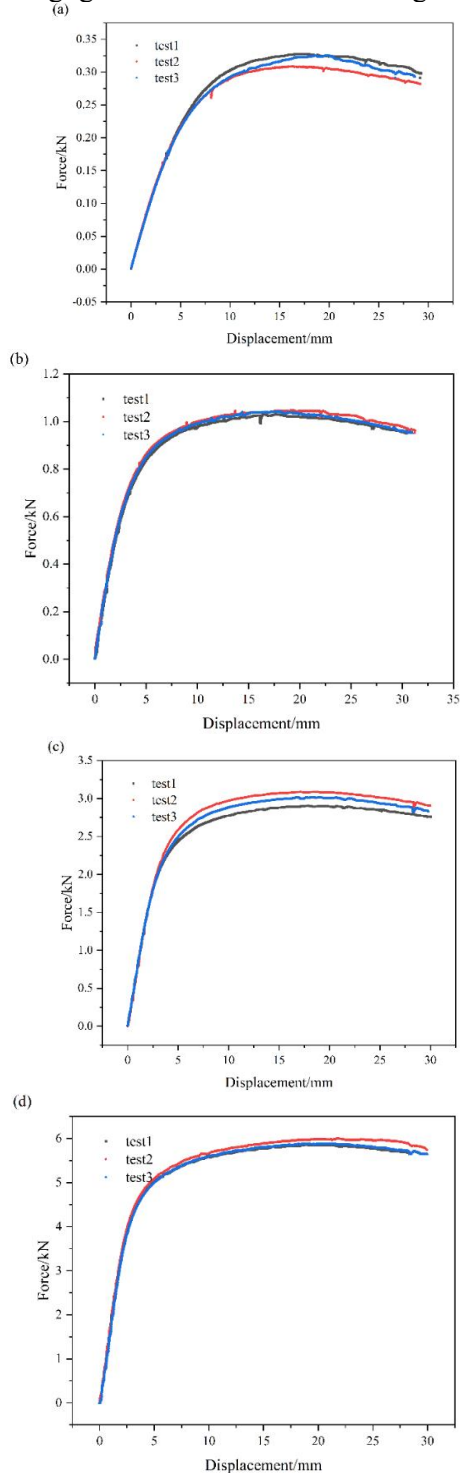
**Figure 3. Stress-Strain Curve of 304 Steel.**

Figure 4 shows the force-displacement curves of the three-point bending test for round bars of 304 steel with different diameters. From the figure, it is evident that the repeatability of the tests is good. The normal force on the indenter increases rapidly with increasing displacement, then gradually slows down and even stabilizes. When the indenter is pressed into a certain displacement, the force increases with the increase of the round bar radius.

Furthermore, comparisons were made between the theoretical bending angles  $\alpha_1$ , residual angles  $\alpha_2$ , and the angle readings  $\alpha_3$  from the inclinometer for round bars of different diameters. The results are shown in Table 1. Where  $\alpha_1$  is calculated based on the pressing depth  $h$  and the distance  $d$  between the two support points in three-point bending, i.e.,  $\alpha_1 = \arctan(2h/d)$ ;  $\alpha_2$  is the bending angle measured directly after unloading.

From Table 1, it can be seen that at a certain displacement load, the inclinometer reading is

approximately consistent with the theoretical bending angle. The round bar with a diameter of 4mm rebounds significantly after unloading, while those with diameters of 6mm and above have negligible rebound after unloading.



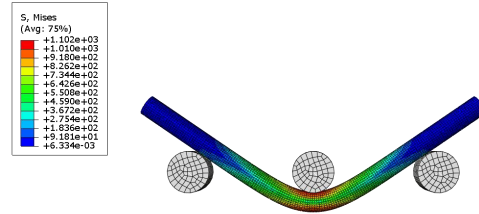
**Figure 4. Force-Displacement Curve of the Three-point Bending Test for 304 Steel Bars of Different Diameters. (a) Diameter 4mm, (b) Diameter 6mm, (c) Diameter 8mm, (d) Diameter 10mm.**

**Table 1. Comparison of Bending Angle Values for 304 Stainless Steel Round Bars of Different Diameters**

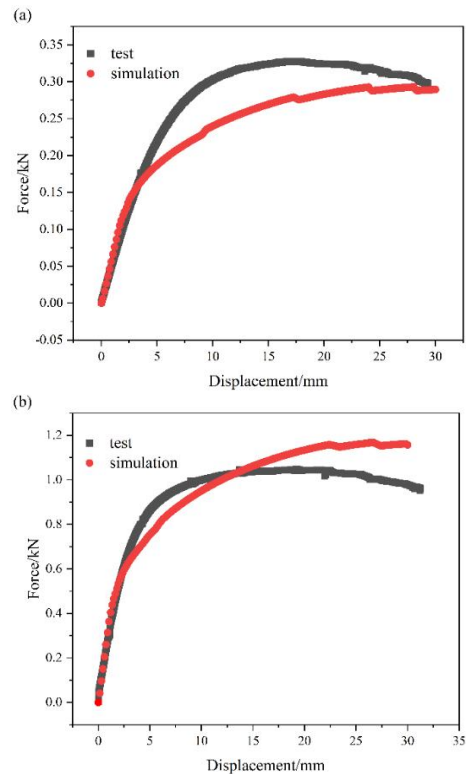
angle type diameter/mm	$\alpha_1$	$\alpha_2$	$\alpha_3$
4	26.56°	19.26	25.40
6	26.56°	25.37	26.20
8	26.56°	26.39	25.45
10	26.56°	26.10	26.45

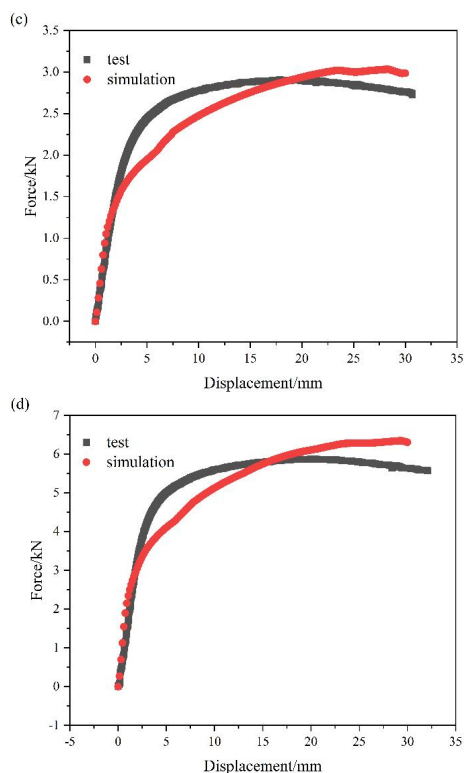
**3.2 Finite Element Results**

Figure 5 below shows the stress cloud diagram of a 10mm diameter 304 stainless steel round bar during three-point bending. The areas with the highest stress can be observed at the point where the indenter contacts the round bar and on the opposite side of the contact region.



**Figure 5. Three-point Bending Simulation Results**





**Figure 6. Comparison of Three-point Bending Test and Finite Element Results for 304 Steel Bars of Different Diameters. (a) Diameter 4mm, (b) Diameter 6mm, (c) Diameter 8mm, (d) Diameter 10mm.**

By comparing the force-displacement curves obtained from the finite element method with the results of the three-point bending test, as shown in Figure 6, it is found that the force-displacement curves output from the finite element simulation match well with the results of the 304 stainless steel three-point bending test.

#### 4. Conclusions

Through three-point bending tests on 304 stainless steel round bars of different diameters, this study analyzed three types of bending angles and compared them with the simulation results from the ABAQUS finite element software. The findings indicate that the diameter of the round bar significantly influences the rebound angle after unloading. Under the same displacement loading conditions, the normal force exerted on the indenter increases with the increase in the diameter of the round bar. The established finite element model considers the material's characteristics and has good accuracy

compared to experimental results.

#### References

- [1] Zhang Zhisheng. (2023) Calculation of Adjustment Values for Reinforced Round Steel Bending Based on the Neutral Layer Principle. *Science and Innovation*, 3, 75-77, 81.
- [2] Xiao, F., Zhang, D.P., Wen, H. and Zhang, D.B. (2013) Development of automated bending production line. *Construction Mechanization*, 7, 62-63.
- [3] Yan, X.S. (2000) Dending Angularity Controlling by Displacement Method. *Physical Testing and Chemical Analysis part A: Physical Testing*, 4, 159-161.
- [4] Chen, Y.H., Zhang, C.P. and Zhu Y.C. (2014) Programming of the Relationship between Head Displacement and Angular in Metallic Materials Bending Test. *Value Engineering*, 22, 25-27.
- [5] Zheng, X.J., Li, Y.P. and Chang, X.H. (2014) Analysis of Rebound Angles Factors for Vertical Bending Steel and Rebound Angle Correction. *Construction Mechanization*, 6, 59-61.
- [6] Hu, S.W., Mi, Z.X., Fan, X.Q. and Lu, J. (2013) A Model for Predicting the Fracture Toughness of Reinforced Concrete Beam in Three-Point Bending. *Journal of Yangtze River Scientific Research Institute*, 30(3), 66-70.
- [7] Wang, Y.H., Fan, J., Zhang, B.F., Wang, G.H. and Yang, X.L. (2023) Experimental Study on Flexural Performance of Polyvinyl Alcohol Fiber Reinforced Composite Beam. *Science Technology and Engineering*, 23(7), 2985-2992.
- [8] Ge, D.L., Li, X.F., Xiao H., Shi L., Han, F. and Chen, J. (2014) Maximum bending angle of UHSS with 1000 MPa strength based on three point bending experiment. *Journal of Plasticity Engineering*, 4, 52-55.
- [9] Cao, H., Huang, L. and Wu, J. (2013) Finite Element Analysis on Bending Performance of Steel Reinforcement Wooden Beams. *Journal of Jiamusi University (Natural Science Edition)*, 31(2), 228-230.
- [10] Hollomon, J.H. (1945) Tensile deformation. *Transactions of the AIME*, 12(4), 1-22.